Advanced Composite Materials
Publication details, including instructions for authors and subscription information:
http://www.tandfonline.com/loi/tacm20

Stiffness and strength of filament-wound fiber-reinforced composite pipes under internal pressure

H. Takayanagi , M. Xia & K. Kemmochi

Version of record first published: 02 Apr 2012.

To cite this article: H. Takayanagi , M. Xia & K. Kemmochi (2002): Stiffness and strength of filament-wound fiber-reinforced composite pipes under internal pressure , Advanced Composite Materials, 11:2, 137-149

To link to this article: http://dx.doi.org/10.1163/156855102760410333

Adv. Composite Mater., Vol. 11, No. 2, pp. 137–149 (2002)

Also available online - www.vsppub.com

Stiffness and strength of filament-wound fiber-reinforced composite pipes under internal pressure

H. TAKAYANAGI[1,*], M. XIA[1] and K. KEMMOCHI[2]

[1] *Smart Structure Research Center (SSRC), National Institute of Advanced Industrial Science and Technology (AIST), AIST Tsukuba Central-4, 1-1-1 Higashi, Tsukuba, Ibaraki 305-8562, Japan*

[2] *Faculty of Textile Science and Technology, Shinshu University, 3-15-1, Tokida, Ueda, Nagano 386-8567, Japan*

Received 31 July 2001; accepted 18 October 2001

Abstract—This paper describes the results of analytical and experimental studies on the rigidity and strength of filament-wound (FW) fiber-reinforced composite pipes under internal pressure. The stiffness, deformation and strength of FW pipes wound at 30°, 45°, 55° and 70°, as well as those of a FW sandwich pipe wound at 55°, were investigated. The experimental strain and displacement for FW pipes wound at 45° and 55° coincided well with the theoretical ones. The experimental strain for FW sandwich pipes was more conservative than the theoretical one. Based on a maximum stress failure criterion, we present a theoretical approach to the prediction of failure strength under internal pressure. Experimental pressure at failure was compared with theoretical loads, and there was a good correlation between the theoretical and experimental results.

Keywords: Maximum stress failure criterion; lamination theory; internal pressure; sandwich cylindrical pipe.

1. INTRODUCTION

Filament-wound (FW) pipes made of fiber-reinforced composites have many potential advantages over pipes made of conventional metal materials. However, the design of FW pipes and, particularly, the prediction of failure strength is complicated because of highly anisotropic material properties. Studies on the mechanical properties and failures of pipes, including bending [1], transverse loading [2, 3], axial compression [4, 5] and internal pressure loading conditions, have been carried out actively.

*To whom correspondence should be addressed. Present address: Dr. Hiroshi Takayanagi, 13-2, Onogawa, Tsukuba-shi, Ibaraki 305-0053, Japan. E-mail: aml05976@mail1.accsnet.ne.jp

Filament-wound fiber-reinforced pipes under internal pressure [6–9] are usually subject to complicated loads involving biaxial or triaxial stresses. For a thin-walled cylindrical pressure vessel, the ratio of applied hoop-to-axial stress is 2 : 1. However, the ratio of hoop-to-axial stress for thick-walled FW pipes will vary with the winding angle. Filament winding provides a means of producing FW pipes in which the fibers can be aligned in preselected directions to carry larger applied loads. Many experimental failure analyses [6, 10–13] have been conducted for thin-walled cylindrical pipes with different winding angles, and an optimum winding angle of 55° has been noted for pipes subjected to internal pressure or biaxial loads with a hoop-to-axial stress ratio of 2 : 1. Rosenow used the classical laminated-plate theory to predict the stress and strain response of pipes with winding angles varying from 15° to 85°, and he compared his predictions to experimental results. A 55° winding angle was shown to be the optimum angle for a FW pipe with a hoop-to-axial stress ratio of 2 : 1, but the optimum angle had to be about 75° in the case of pressure without axial loading. Uemura and Fukunaga [8] and Spencer and Hull [14] have investigated, respectively, the failure mechanism in glass fiber-reinforced plastic pipes and in carbon fiber-reinforced plastic pipes wound at different winding angles. The negative axial strains were observed within a range of 35° to 50° because of the effect of anisotropic elasticity on the axial strain. The elastic properties of FW pipes were measured using strain gauges, and fracture mechanisms were obtained from photographs. The experimental results showed that the deformation and failure mechanisms of FW pipes were strongly dependent on winding angles.

The highly specific strength and good corrosion resistance of fiber-reinforced plastic pipes have led to an increase in their use in the chemical and other industries in recent years. However, there have been few investigations on the mechanical properties of FW pipes under internal pressure and, particularly, there is almost no literature on the properties of thick-walled FW sandwich pipes. In the present paper, we report experimental and theoretical investigations carried out for the stiffness and the deformation properties of FW pipes under internal pressure. A theoretical approach to the prediction of failure strength for FW pipes is presented based on a maximum stress failure criterion. The experimental and theoretical investigation revealed the failure modes of FW pipes under internal pressure.

2. STRESS AND DEFORMATION ANALYSES [9]

It is well known that hoop stress is twice the axial stress for a thin-walled pressure cylinder with closed ends. However, it is necessary to design a relatively high thickness-to-radius ratio when a pipe is subjected to greater pressure. For thick-walled FW pipes, the stresses and strains become more complicated because of anisotropic properties. The ratio of hoop-to-axial strain will vary with the winding angle. Xia *et al.* [9] have developed an analytical procedure to assess the stresses and deformations of thick-walled FW sandwich pipes under internal pressure.

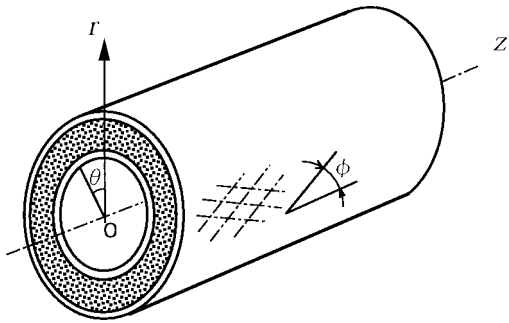

Figure 1. Filament-wound sandwich pipe in cylindrical coordinates.

Figure 1 shows the cylindrical coordinate for a FW sandwich pipe. The stresses and strains are independent of the winding angle ϕ, and there is no shear-extension coupling. Therefore, the equilibrium equation for stress of the kth layers is

$$\frac{\mathrm{d}\sigma_r^{(k)}}{\mathrm{d}r} + \frac{\sigma_r^{(k)} - \sigma_\theta^{(k)}}{r} = 0. \tag{1}$$

The radial and hoop strains, $\varepsilon_r^{(k)}$ and $\varepsilon_\theta^{(k)}$, can be given in the radial displacement $u_r^{(k)}$ by

$$\varepsilon_r^{(k)} = \frac{\mathrm{d}u_r^{(k)}}{\mathrm{d}r} \quad \text{and} \quad \varepsilon_\theta^{(k)} = \frac{u_r^{(k)}}{r}. \tag{2}$$

The axial strains $\varepsilon_z^{(k)}$ of all layers are equal to a constant, ε_0.

The radial stress $\sigma_r^{(k)}$, the hoop stress $\sigma_\theta^{(k)}$ and the axial stress $\sigma_z^{(k)}$ can be expressed in terms of strains

$$\begin{Bmatrix} \sigma_r \\ \sigma_\theta \\ \sigma_z \end{Bmatrix}^{(k)} = \begin{bmatrix} C_{11} & C_{12} & C_{13} \\ C_{12} & C_{22} & C_{23} \\ C_{13} & C_{23} & C_{33} \end{bmatrix}^{(k)} \begin{Bmatrix} \varepsilon_r \\ \varepsilon_\theta \\ \varepsilon_z \end{Bmatrix}^{(k)}, \tag{3}$$

where $[C_{ij}]^k$ are the off-axis stiffness constants, which can be calculated from the on-axis stiffness constants by using the stiffness transformation matrix. 1, 2 and 3 represent the r, θ and z directions, respectively.

Substituting equation (3) for the stresses into equation (1) and using equation (2), we get the differential equation of the radial displacement, given by

$$\frac{\mathrm{d}^2 u_r^{(k)}}{\mathrm{d}r^2} + \frac{1}{r}\frac{u_r^{(k)}}{\mathrm{d}r} - \frac{C_{22}^{(k)}/C_{11}^{(k)}}{r^2} u_r^{(k)} = \frac{C_{23}^{(k)} - C_{13}^{(k)}}{C_{11}^{(k)}} \frac{\varepsilon_0}{r}. \tag{4}$$

Based on the solution of equation (4), the strain and the stress can be obtained from equations (2) and (3).

3. EXPERIMENTAL

3.1. Materials and sample preparation

The resin was vinyl ester (UE-5210) supplied by Dainippon Ink and Chemicals, Co., Ltd. Immediately prior to winding, a resin bath containing 100 parts by weight resin, 2 parts additive (RS-406), 0.4 parts promoter (cobalt naphthenate) and 0.8 parts curing agent (Permec N) was prepared. FW pipes were wound using glass fiber roving (RS110PE535) at winding angles of 30°, 45°, 55° and 70° at Nittobo FRP Laboratory Co., Ltd. The FW pipes had an inside radius of 50 mm and an alternate-ply layer thickness of 2 mm.

FW sandwich pipes were fabricated using alternate-ply material wound at 55° for the skin layers and polyurethane foam with a 20 mm thickness for the core layer. The pipes had an inside radius of 50 mm and an outside radius of 74 mm. The length of all the pipes was 900 mm. The pipes were cured at room temperature.

The properties of the skin layers were obtained from the unidirectionally wound (UD) laminates with the same fiber content as that of the skin layers. The properties of the UD laminates and polyurethane foam, measured using an Instron universal testing machine, are shown in Table 1. The fiber volume fraction of the skin layers was 47%.

3.2. Test methods

Pipe strength under internal pressure was investigated by using an internal pressure test apparatus made by Intesco Co., Ltd. In all of the tests, the hydraulic chamber pressure was increased at a steady rate. For the FW pipes, the internal pressurization rate was 2 MPa/min, and the FW sandwich pipe was subjected to increasing pressure at a rate of 10 MPa/min. The strains were measured with

Table 1.
Properties of UD laminates and plastic foam

Properties		UD laminates	Foam material
Tensile strength (MPa)	0°-direction	1000	
			—
	90°	21.4	
Compressive strength (MPa)	0°	504	
			0.33
	90°	105	
Shear strength (MPa)	0°–90°	19.2	—
Tensile modulus (GPa)	0°	39.4	
			0.0078
	90°	8.26	
Shear modulus (GPa)	0°–90°	5.47	0.003
Poisson's ratio	0°	0.309	0.3

strain gages bonded to the surface of the central parts of the pipes along the hoop and axial directions, and the radial deformations were measured with displacement transducers.

4. RESULTS AND DISCUSSION

4.1. Stiffness and deformation

Figures 2 to 4 show the strain and displacement per unit of internal pressure (MPa) of the FW pipes at different winding angles. From these figures, the effects of

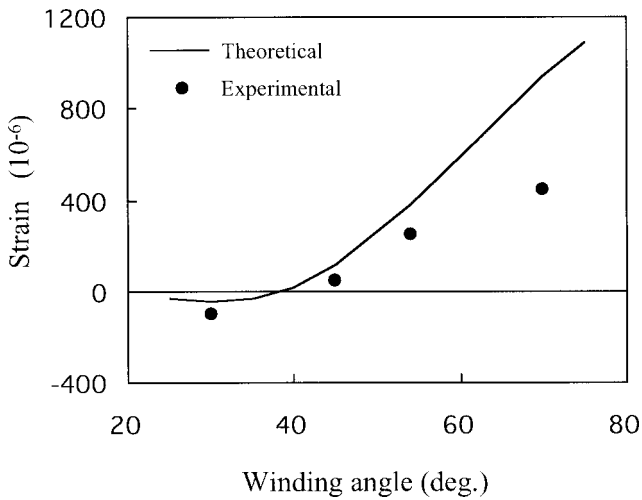

Figure 2. Effect of the winding angle on strain in the axial direction.

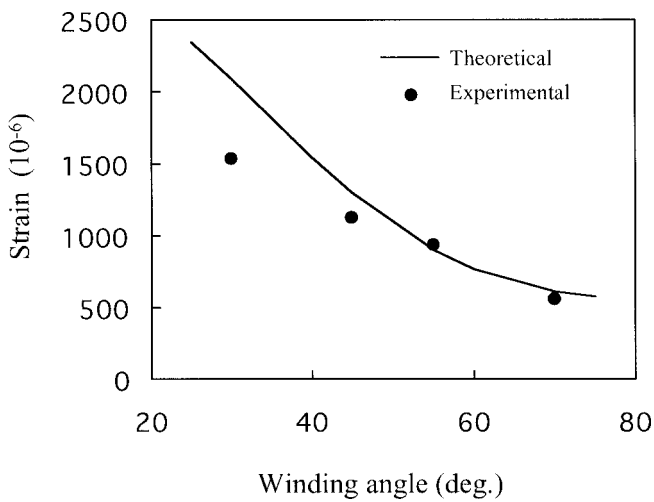

Figure 3. Effect of the winding angle on strain in the hoop direction.

winding angle on strain and displacement were observed, and comparisons between the theoretical and experimental values were made. As shown in Figs 2 and 3, the axial strain increased and the hoop strain decreased when the winding angle was increased. For the FW pipe with a winding angle of 30°, the results obtained from both the calculation and the experiment exhibit a negative axial strain because greater hoop strain occurs in the circumference. The radial displacement decreased as the winding angle was increased, as shown in Fig. 4. There is a good correlation between the theoretical and experimental strain and displacement for FW pipes wound at 45° and 55°.

The theoretical axial and hoop strains based on the present theory and the experimental ones per unit of internal pressure (MPa) of the FW sandwich pipe are summarized in Table 2. The experimental strains were more conservative than the theoretical ones. It was considered for the above reason that the stiffness of the core layer was extremely less than that of the skin layers.

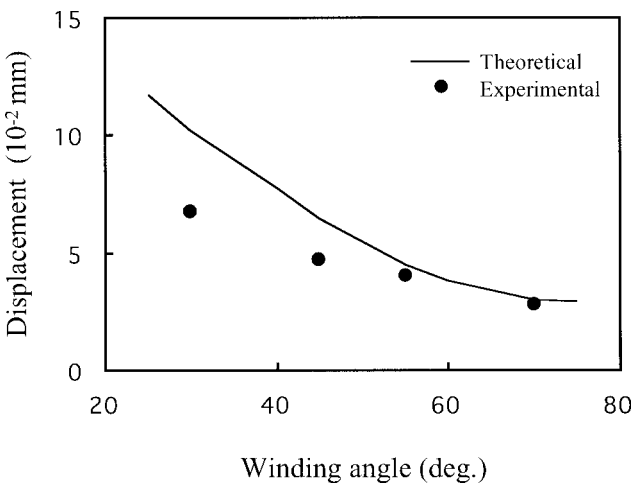

Figure 4. Effect of the winding angle on displacement.

Table 2.
Axial and hoop strains: results of filament-wound sandwich pipe

		Experimental	Theoretical	Exp./Theor.
Strain (10^{-6})	Axial	91.9	156	0.6
	Hoop	−11.2	−16.5	0.7
Failure pressure (MPa)		5.2*	4.6	1.1

* Failure pressure in inner layer.

4.2. Strength and failure

Transverse tensile stresses normal to the fibers cause debonding at the fiber/matrix interface and resin cracking parallel to the fibers. Tensile stresses along the fiber direction cause fiber breakage, and shear stresses produce shear failure along the interface between the matrix and fibers.

The longitudinal tensile stress σ_L, the transverse tensile stress σ_T and the maximum shear stress τ_{LT} can be given by [15]

$$\begin{aligned}
\sigma_L &= \sigma_z \cos^2\phi + \sigma_\theta \sin^2\phi + (\sigma_z\chi_0 + \sigma_\theta\psi_0)G_{z\theta}\sin 2\phi,\\
\sigma_T &= \sigma_z \sin^2\phi + \sigma_\theta \cos^2\phi - (\sigma_z\chi_0 + \sigma_\theta\psi_0)G_{z\theta}\sin 2\phi,\\
\tau_{LT} &= \max_\beta\left\{\sqrt{\tau_{z'\theta'}^2 + \tau_{\theta'r'}^2}\right\},
\end{aligned}$$

and

$$\begin{aligned}
\tau_{z'\theta'} &= -\sigma_z \sin\beta\cos\beta + \sigma_\theta \sin\beta\cos\beta\cos^2\alpha + (\sigma_z\chi_0 + \sigma_\theta\psi_0)G_{z\theta}\cos 2\beta\cos\alpha,\\
\tau_{\theta'r'} &= -\sigma_\theta \cos\beta\sin\alpha\cos\alpha + (\sigma_z\chi_0 + \sigma_\theta\psi_0)G_{z\theta}\sin\beta\sin\alpha,
\end{aligned}$$

$$\begin{aligned}
\chi_0 &= \left[\frac{\sin^2\phi}{E_T} - \frac{\cos^2\phi}{E_L} + \frac{1}{2}\left(\frac{1}{G_{LT}} - \frac{2\nu_L}{E_L}\right)\cos 2\phi\right]\sin 2\phi,\\
\psi_0 &= \left[\frac{\cos^2\phi}{E_T} - \frac{\sin^2\phi}{E_L} - \frac{1}{2}\left(\frac{1}{G_{LT}} - \frac{2\nu_L}{E_L}\right)\cos 2\phi\right]\sin 2\phi,\\
\frac{1}{G_{z\theta}} &= \left(\frac{1+\nu_L}{E_L} + \frac{1+\nu_T}{E_T}\right)\sin^2 2\phi + \frac{1}{G_{LT}}\cos^2 2\phi,
\end{aligned} \tag{5}$$

$$\begin{aligned}
\cos\alpha &= \tan\beta/\tan\phi,\\
\cos\varphi &= \cos\phi/\cos\beta,\ (\beta \leqslant \phi),
\end{aligned}$$

where β is the angle between the shear plane and the cylindrical axis z. E_L and E_T are the longitudinal and transverse Young's modulus, respectively.

According to the maximum stress criterion, failure occurs under one of the following three conditions:

(1) The tension failure caused by fiber fractures:

$$\sigma_L \geqslant F_L \quad \text{or} \quad \sigma_L \leqslant -F'_L,$$

(2) The separation failure between the fibers and the matrix, or the failure of the matrix itself:

$$\sigma_T \geqslant F_T \quad \text{or} \quad \sigma_T \leqslant -F'_T,$$

(3) The shear failure along the interface between the matrix and the fibers:

$$\tau_{LT} \geqslant F_{LT} \quad \text{or} \quad \tau_{LT} \leqslant -F_{LT},$$

where F and F' are the tensile and compressive strengths, respectively. Subscripts L and T refer to directions parallel to and perpendicular to the fibers, respectively. F_{LT} is the shear strength.

Figures 5 and 6 show the variation of stresses at the inner surface with the winding angle for a FW pipe and the FW sandwich pipe, respectively. The maximum tensile stresses in the fiber direction are about 55°. For the FW pipe, the minimum transverse tensile stress (σ_T) normal to the fibers is about 55°; for the FW sandwich pipe, it is about 60°. Based on netting analysis, it has been reported by Xia *et al.* [9] that the optimal winding angles are in the 60° range for a FW sandwich pipe.

Figure 7 shows the stress–strain curves of FW pipes wound at winding angles of 30°, 45°, 55° and 70°. This figure is plotted against the measured strains in the

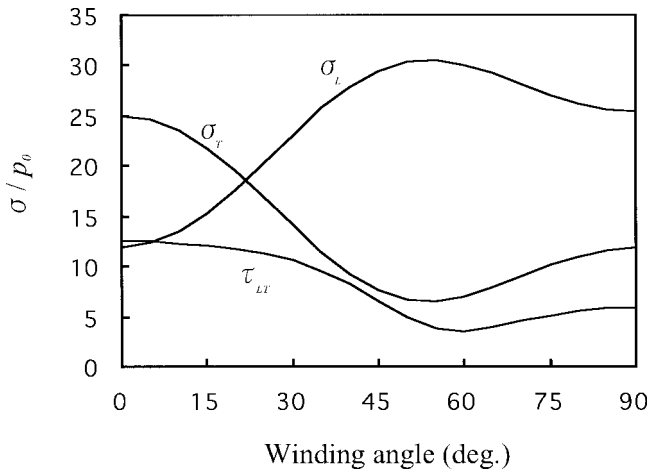

Figure 5. Effect of the winding angle of FW pipe on stresses related to the fiber direction.

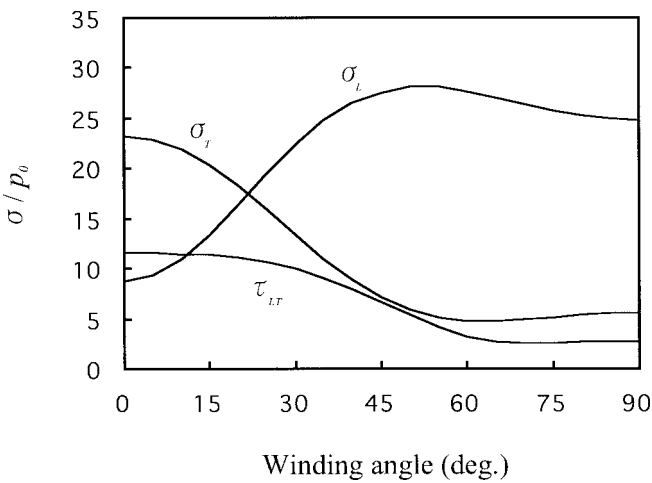

Figure 6. Effect of the winding angle of FW sandwich pipe on stresses related to the fiber direction.

hoop and axial directions, indicated by H and A, respectively. All pipes showed initial linear elastic properties. The slope $\sigma_\theta/\varepsilon_\theta$ (hoop stiffness) increased as the winding angle increased, whereas the slope $\sigma_\theta/\varepsilon_z$ decreased with the winding angle and was negative for the FW pipe wound at 30°.

The FW pipes with winding angles of 30° and 70° showed brittle breaking behavior. It was observed that only small amounts of initial weepage occurred at the pipe surface, and then burst fractures occurred. Figure 8 shows photographs of FW pipes after the fractures. Local whitening of pipes wound at 30° and 70° can be observed in Fig. 8a and d, respectively. The cracks occurred in the directions of the fiber orientation.

The fracture of a FW pipe wound at 55° showed no brittle behavior. Weepage occurred at a pressure corresponding to hoop stress between 142 and 170 MPa. Then a large amount of leakage occurred, and the pipe underwent failure. It is shown in Fig. 8c that a few cracks occurred parallel to the fibers.

The stress–strain curve of the pipe wound at 45° showed a larger nonlinear property and had a smooth variation. The axial strain was positive at the initial state and became negative when the strain continued to be increased. This was because hoop strain increases rapidly as internal pressure is increased. Weepage occurred at a pressure corresponding to hoop stress after about 82 MPa. The weepage was small droplets on the whole surface of the pipe, and there was not a large amount of local leakage or sharp breakage. As shown in Fig. 8b, the whitening developed uniformly throughout the pipe, and an interlaminar shear fracture can be seen.

The variation of the burst strength for FW pipes with the winding angle is shown in Fig. 9. An experimental investigation was compared to the results of theoretical calculations. The burst strength can be predicted based on the maximum stress criterion. In Fig. 9, P_L, P_T and P_{LT} are simulated curves of the maximum internal

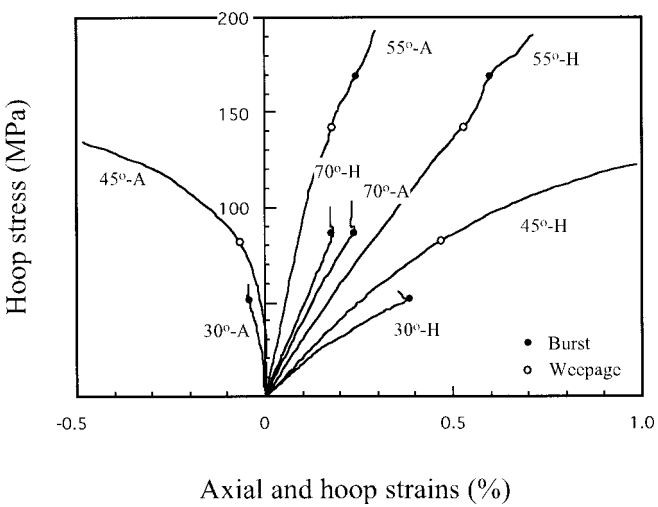

Figure 7. Stress–strain curves of FW pipes under internal pressure.

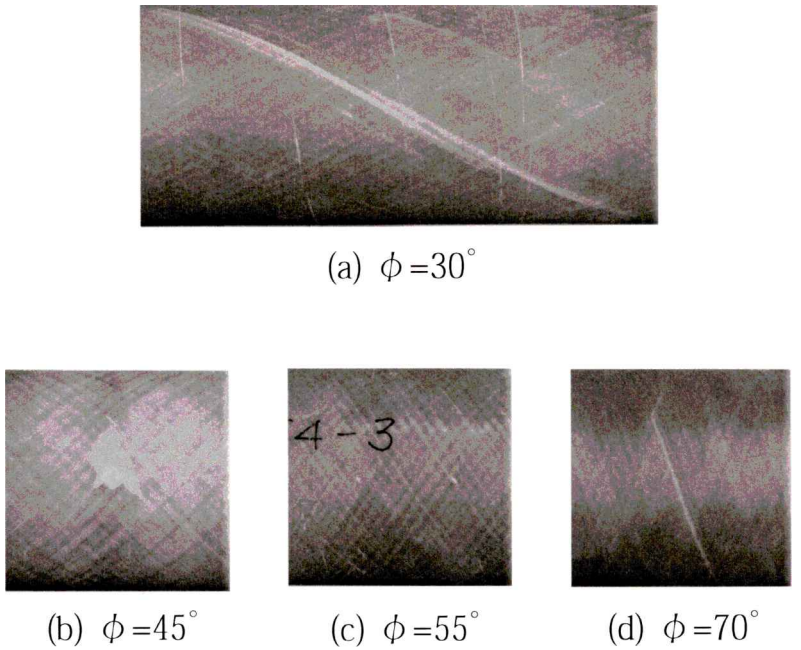

Figure 8. Failure mode of FW pipes.

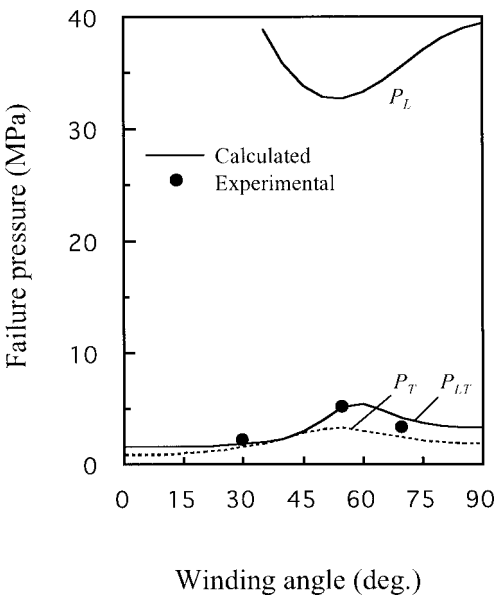

Figure 9. Variation of the failure strength for FW pipes with the winding angle.

pressures caused by the longitudinal, transverse and the shear failures, respectively. The FW pipe failures were not caused by the fiber fracture because there was significant tensile strength in the fiber direction. For the pipes with winding angles of 30° and 70°, the failures were caused by separation failures between the fibers and the matrix. Pipes with a winding angle of 55° were subject to shear failure. Because the pipes were made with multiple layers, the fiber separation failures on a layer could be reinforced by the closely bounded layer with the opposite fiber orientation angle. The optimal winding angle of FW pipes subjected to the maximum internal pressure was found to be around 55°. There was a good correlation between the experimental pressure at failure and the theoretical one.

The calculated and experimental failure pressure of a FW sandwich pipe wound at 55° is summarized in Table 2. The curves of internal pressure versus strain of the pipe are shown in Fig. 10. Weepage was not observed from the outer surface of the sandwich pipe. The initial weepage occurred in the inner layer when the internal pressure continued to be increased to about 5.2 MPa. As shown in Fig. 10, the variation of the internal pressure with strains caused greater non-elastic behavior. It was observed that a large amount of the weepage at the inner layer occurred at a pressure of about 7.4 MPa. A large mount of water poured into the pipe but was absorbed by the low-density foam material. Pressure at failure of FW sandwich pipe was slightly larger than FW pipe wound at 55°. That was because the rigidity of the plastic foam was much less than that of the alternate-ply material. Figure 11 is a photograph of a failure in the inner layer of the FW sandwich pipe. A crack in the resin and the matrix/fibers interface is shown in the cross-sectional photograph of the pipe.

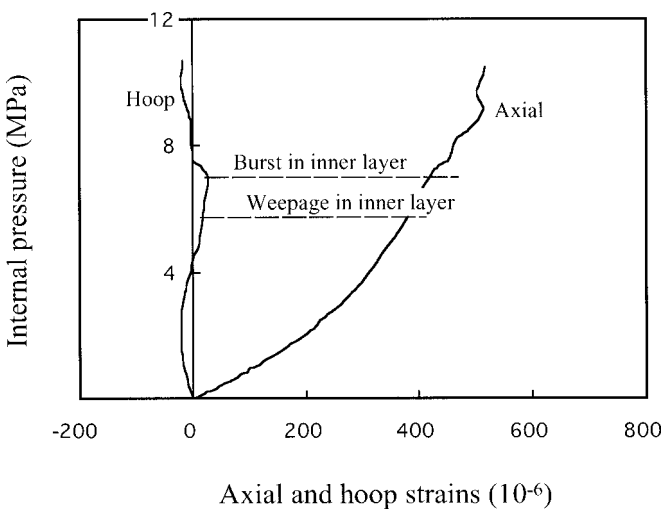

Figure 10. Curves of internal pressure versus strains of FW sandwich pipe.

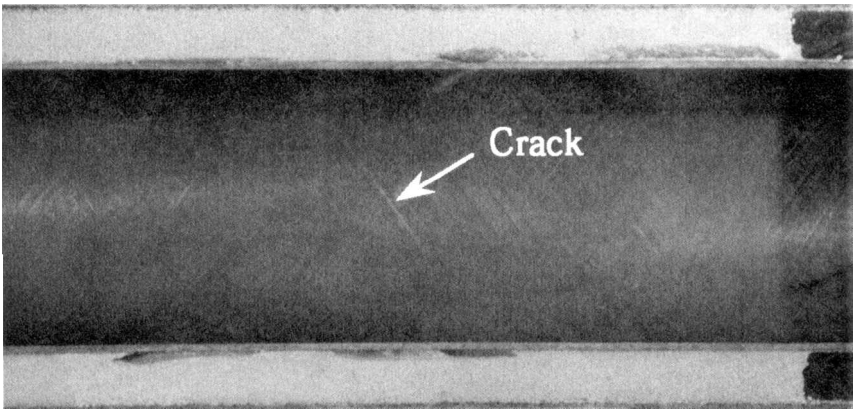

Figure 11. Failure mode of FW sandwich pipe.

5. CONCLUSIONS

Experimental and theoretical investigations were carried out to evaluate the rigidity and strength of FW composite pipes under internal pressure. The experimental strain and displacement for FW pipes wound at 45° and 55° coincided well with the theoretical ones. The experimental strain of FW sandwich pipe was more conservative than the theoretical one. It was considered for the above reason that the stiffness of the core layer was much less than that of the skin layer.

The FW pipes with winding angles of 30° and 70° showed brittle breaking behaviors caused by transverse tensile stresses. The FW pipe wound at 55° was subjected to shear fracture and showed the maximum internal pressure load. The failure strength of FW pipes can be predicted based on the maximum stress failure criterion. Pressure at failure of FW sandwich pipe was slightly larger than FW pipe wound at 55°. That was because the rigidity of the plastic foam was much less than that of the alternate-ply material.

REFERENCES

1. N. Akkus and M. Kawahara, Bending behaviors of thin composite pipes with reinforcing nodes, *Materials Science Research International* **6**, 131–135 (2000).
2. K. L. Alderson and K. E. Evans, Failure mechanisms during the transverse loading of filament-wound pipes under static and low velocity impact conditions, *Composites* **23**, 167–173 (1992).
3. T. Nishiwaki, A. Yokoyama, Z. Maekawa, H. Hamada and S. Mori, A quasi-three-dimensional lateral compressive analysis method for a composite cylinder, *Compos. Struct.* **32**, 293–298 (1995).
4. Y. Onoda, Optimal laminate configurations of cylindrical shells for axial buckling, *AIAA J.* **23** (7), 1093–1098 (1985).
5. A. A. Smerdov, A computational study in optimum formulations of optimization problems on laminated cylindrical shells for buckling: I. Shells under axial compression, *Compos. Sci. Technol.* **60**, 2057–2066 (2000).

6. D. Hull, M. J. Legg and B. Spencer, Failure of glass/polyester filament wound pipe, *Composites* **9**, 17–24 (1978).
7. K. Kitao and H. Akiyama, Failure of thick-wall filament wound plastic pipes under internal pressure, *J. Soc. Mater. Sci., Japan* **43**, 1134–1140 (1994) (in Japanese).
8. M. Uemura and H. Fukunaga, Probabilistic burst strength of filament-wound cylinders under internal pressure, *J. Compos. Mater.* **15**, 462–480 (1981).
9. M. Xia, K. Kemmochi and H. Takayanagi, Analysis of filament-wound sandwich pipe under internal pressure, *Adv. Composite Mater.* **9**, 223–239 (2000).
10. F. Ellyin, M. Carroll, D. Kujawski and A. S. Chiu, The behavior of multidirectional filament wound fibreglass/epoxy tubulars under biaxial loading, *Composites* **28A**, 781–790 (1997).
11. P. D. Soden, D. Leadbetter, P. R. Griggs and G. C. Eckold, The strength of a filament wound composite under biaxial loading, *Composites* **9**, 247–250 (1978).
12. P. D. Soden, R. Kitching and P. C. Tse, Experimental failure stresses for $\pm 55^\circ$ filament wound glass fiber reinforced plastic tubes under biaxial loads, *Composites* **20**, 125–135 (1989).
13. M. W. K. Rosenow, Wind angle effects in glass fiber-reinforced polyester filament wound pipes, *Composites* **15**, 144–152 (1984).
14. B. Spencer and D. Hull, Effect of winding angle on the failure of filament wound pipe, *Composites* **9**, 263–271 (1978).
15. K. Yamawaki and M. Uemura, Fracture strength of helically wound composite cylinder, II Torsional strength, *J. Soc. Mater. Sci., Japan* **21**, 330–336 (1972) (in Japanese).